

UDC 666.3 + 544.01

DOI dx.doi.org/10.17073/1997-308X-2022-3-55-62

Refinement of the eutectic composition in the $\text{LaB}_6\text{--VB}_2$ system

© 2022 г. **E.S. Novoselov¹, V.I. Almjashев², D.D. Nesmelov¹, D.P. Danilovich¹**

¹ Saint-Peterburg State Institute of Technology (SPSIT), Saint-Petersburg, Russia

² Alexandrov NITI, Leningrad Region, Sosnovy Bor, Russia

Received 29.04.2022, revised 14.07.2022, accepted for publication 18.07.2022

Abstract: The $\text{LaB}_6\text{--VB}_2$ alloy with the eutectic structure was obtained by cold crucible induction melting followed by crystallization. The mole ratio of components in the initial powder mixture was 35 : 65. The structure and composition of the $\text{LaB}_6\text{--VB}_2$ material were studied by X-ray diffraction, scanning electron microscopy, and X-ray microanalysis. The composition of the alloy is represented by two boride phases — cubic LaB_6 and hexagonal VB_2 . Two-phase eutectic regions up to 500 μm in size represent a LaB_6 matrix filled with 0.8–2.0 μm thick VB_2 fibers (filamentary, rod crystals). VB_2 fibers are predominantly oriented along the direction of the temperature gradient that appeared when cooling the melt, i.e. from the outer surface of the sample to its center. The integrated phase area analysis was used to determine the eutectic composition: $42 \pm 1 \text{ mol\% LaB}_6$ and $58 \pm 1 \text{ mol\% VB}_2$.

Keywords: lanthanum hexaboride, vanadium diboride, eutectic, cold crucible method, anisotropy.

Novoselov E.S. – Engineer, Department of chemical technology of high-melting and silicate materials (CTHSM), Saint-Peterburg State Institute of Technology (SPSIT) (190013, Russia, Saint-Petersburg, Moskovskii pr., 26).
E-mail: lehmann330@gmail.com.

Almjashev V.I. – Head of the Severe Accidents Research Department, Alexandrov NITI (188540, Russia, Leningrad Reg., Sosnovyj Bor, Koporskoe sh., 72). E-mail: vac@mail.ru.

Nesmelov D.D. – Associated professor, Department of CTHSM, SPSIT.
E-mail: dnesmelov@yandex.ru.

Danilovich D.P. – Associated professor, Department of CTHSM, SPSIT.
E-mail: dmitrydanilovich@gmail.com.

For citation: Novoselov E.S., Almjashev V.I., Nesmelov D.D., Danilovich D.P. Refinement of the eutectic composition in the $\text{LaB}_6\text{--VB}_2$ system. *Izvestiya Vuzov. Poroshkovaya Metallurgiya i Funktsional'nye Pokrytiya (Powder Metallurgy and Functional Coatings)*. 2022. Vol. 16. No. 3. P. 55–62 (In Russ.).
DOI: dx.doi.org/10.17073/1997-308X-2022-3-55-62.

Уточнение эвтектического состава в системе $\text{LaB}_6\text{--VB}_2$

Е.С. Новоселов¹, В.И. Альмяшев², Д.Д. Несмелов¹, Д.П. Данилович¹

¹ Санкт-Петербургский государственный технологический институт (технический университет) (СПбГТИ (ТУ)), г. Санкт-Петербург, Россия

² Научно-исследовательский технологический институт (НИТИ) им. А.П. Александрова, г. Сосновый Бор, Ленинградская обл., Россия

Статья поступила в редакцию 29.04.2022 г., доработана 14.07.2022 г., подписана в печать 18.07.2022 г.

Аннотация: Сплав с эвтектической структурой системы $\text{LaB}_6\text{--VB}_2$ был получен индукционной плавкой методом холодного тигля с последующей кристаллизацией. Мольное соотношение компонентов в исходной порошковой смеси составляло 35 : 65. Методами рентгеновской дифракции, сканирующей электронной микроскопии и микрорентгеноспектрального анализа исследованы структура и состав материала $\text{LaB}_6\text{--VB}_2$. Состав сплава представлен двумя фазами боридов — кубическим LaB_6 и гексагональным VB_2 . Двухфазные эвтектические области размером до 500 мкм представляют собой

матрицу LaB_6 , наполненную волокнами VB_2 (нитевидными, стержневыми кристаллами) толщиной 0,8–2,0 мкм, которые преимущественно ориентированы вдоль направления температурного градиента, возникшего при охлаждении расплава, т.е. от внешней поверхности образца к его центру. С помощью метода анализа интегральной площади фаз установлен состав эвтектики: 42 ± 1 мол. % LaB_6 и 58 ± 1 мол. % VB_2 .

Ключевые слова: гексаборид лантана, диборид ванадия, эвтектика, метод холодного тигля, анизотропия.

Новоселов Е.С. – инженер кафедры химической технологии тугоплавких неметаллических и силикатных материалов (ХТНСМ), СПбГТИ (ТУ) (190013, г. Санкт-Петербург, Московский пр-т, 26).

E-mail: lehmann330@gmail.com.

Альмяшев В.И. – начальник отдела исследований тяжелых аварий, НИТИ им. А.П. Александрова (188540, Ленинградская обл., г. Сосновый Бор, Копорское шоссе, 72).

E-mail: vac@mail.ru.

Несмелов Д.Д. – доцент кафедры ХТНСМ, СПбГТИ (ТУ).

E-mail: dnesmelov@yandex.ru.

Данилович Д.П. – доцент кафедры ХТНСМ, СПбГТИ (ТУ).

E-mail: dmitrydanilovich@gmail.com.

Для цитирования: Новоселов Е.С., Альмяшев В.И., Несмелов Д.Д., Данилович Д.П. Уточнение эвтектического состава в системе $\text{LaB}_6\text{--VB}_2$. Известия вузов. Порошковая металлургия и функциональные покрытия. 2022. Т. 16. № 3. С. 55–62. DOI: dx.doi.org/10.17073/1997-308X-2022-3-55-62.

Introduction

Materials using quasi-binary systems containing rare-earth metal hexaborides (primarily LaB_6) and transition metal diborides (MB_2 , where M can be Ti, Zr, Hf, Ta, Nb, V, Cr, W, and Mo) have been the focus of research for decades due to their outstanding thermal emission properties [1–4]. When compared to poly- or single-crystal LaB_6 commonly used for making thermal emission cathodes, materials based on $\text{LaB}_6\text{--MB}_2$ eutectic systems have a lower work function and higher emission current density at the same operating temperature. Studies [2, 5, 6] show that the cathode manufacturing process significantly affects its thermal emission properties: directionally crystallized cathodes made from $\text{LaB}_6\text{--VB}_2$ and $\text{LaB}_6\text{--ZrB}_2$ systems have higher emission currents than their sintered polycrystalline analogs. The directionally crystallized cathode materials manufactured by zone melting have a two-phase structure. The LaB_6 matrix phase is regularly «reinforced» by rod-like or plate crystals of the diboride phase.

Better thermal emission properties associated with the formation of such a structure are of great importance for thermocathode materials. There is also another effect applicable to a wider range of materials. It occurs in directionally crystallized materials made from $\text{LaB}_6\text{--MB}_2$ systems and results in a significant

increase in their physical and mechanical properties compared to their monocrystalline and sintered analogs [7–13].

In order to create materials using $\text{LaB}_6\text{--MB}_2$ eutectic systems, reliable data on the phase equilibria in such systems, their composition, and eutectic temperature are required [14–23]. Experimental measurements of these properties in high-temperature oxygen-free systems are technically challenging, so the available literature is sparse. Furthermore, such data has to be verified, since it was obtained using outdated techniques. For example, [14, 15] report contradictory eutectic properties for LaB_6 and VB_2 . A possible reason is a molar to a mass concentration conversion error.

This study aims to obtain a more precise eutectic composition of the $\text{LaB}_6\text{--VB}_2$ system experimentally. Another goal is to make eutectic compositions by induction melting without special directional crystallization equipment. It is of practical interest since industrial-grade induction melting is more affordable compared with zone melting. In contrast, induction melting does not guarantee identical temperature gradients across the material volume. Therefore, the assessment of the structure regularity (when a continuous eutectic structure or individual eutectic regions with different orientations are formed) is of particular interest.

Methods

We made lanthanum and vanadium borides by means of the borothermal reduction of oxides using commercially available La_2O_3 (99.99 % purity), V_2O_5 (99.0 %), and amorphous boron (99.0 %) powders. A vacuum resistance furnace at 1650 °C (LaB_6) and 1200 °C (VB_2) was used. The isothermal hold time was 1 h at 10^{-1} Pa residual gas pressure.

The average particle size of the LaB_6 and VB_2 powders measured by laser diffraction was 5 to 10 μm . The powders contained only the target phases (cubic LaB_6 and hexagonal VB_2) without the initial components or any other crystalline phases. Elemental analysis indicated the presence of oxygen adsorbed at the particle surface, amounting to 1.2 wt.%. We used a Union Process HD-1 attritor (Union Process, USA) with silicon carbide grinding bodies for mixing and grinding the powders to a 1.5 μm average particle size for 6 h in the BR-1 solvent (gasoline). About 0.7 wt.% SiC was added to the mixture due to the wear of the grinding bodies.

The concentration of the mixture components was selected to match the eutectic point, as reported in [14, 15]. Ordanyan S. [14] specifies the molar content of VB_2 in the eutectic as 69 mol.%, which corresponds to 44 wt.% mass concentration of VB_2 . However, according to [14, 15] the mass content of VB_2 is 40 wt.%. This discrepancy may be a result of a concentration conversion error in [14], so we opted for a VB_2 40 wt.% (65 mol.%) experimental mixture.

After drying, the powder was compacted into cylinders 40 mm dia. and 40 mm high using a hydraulic press. Rasplav 2 and Rasplav 3 furnaces (made in Russia) were used for induction melting of the samples. We applied the cold-crucible technology in an argon flow described in [22].

The resulting crystallized ingot was cut in two mutually perpendicular directions using a diamond cutting disc.

The microstructure of the polished sections was analyzed with a Tescan Vega 3SBH scanning electron microscope (SEM) (Czech Republic).

We used a Rigaku SmartLab 3 multipurpose diffractometer (Japan) in the $2\theta = 10^\circ \div 80^\circ$ angular range ($\text{Cu}K_\alpha$ radiation, Ni filter, 0.01° scan step) for X-ray phase analysis of the initial components, powders, and

crystallized alloys. The phase composition and lattice cell properties were estimated with the SmartLab Studio 3 software and the ICDD PDF-2 diffraction database.

The concentration of components in the eutectic alloy was estimated by means of three alternative methods:

- SEM-EDX elemental composition analysis with an Aztec X-Act X-ray energy dispersive spectroscopy analyzer (Oxford Instruments, UK);

- FP XRD analysis with the SmartLab Studio 3 software;

- IAP was applied to the SEM images of the polished sections using the Thixomet Lite software package (Russia).

Results and discussion

Fig. 1 shows the results of the LaB_6 — VB_2 crystallized alloy SEM analysis. The alloy consists mainly of extensive (up to 500 μm) two-phase eutectic regions where the hexagonal VB_2 fibers (filamentary, rod-like crystals extended along the C crystallographic axis) are located in the LaB_6 matrix (Fig. 1, a, b). The VB_2 fibers are predominantly oriented along the temperature gradient created during the melt cooling, i.e., from the outer surface of the sample to its central region. However, there are local deviations from the predominant direction (Fig. 1, c). The degree of structure regularity is lower than that of zone-melting materials [2–13] as was expected.

However, in comparison with the LaB_6 — NbB_2 — W_2B_5 alloy that we obtained earlier by electric arc melting [23], in the LaB_6 — VB_2 made by the cold-crucible technology, the arrangement of the eutectic regions is more ordered. Depending on the melt local cooling rate, the diameter of the VB_2 fibers varies from 0.8 to 2.0 μm . Fibers over 2 μm tend to merge (Fig. 1, d). In some cases, probably where the specified concentration was disturbed due to imperfect mixing, large (up to 100 μm) single-phase VB_2 areas with prominent rounded contours were formed (Fig. 1, e). Besides the deviations in concentration, this could be caused by the presence of vanadium oxide impurities on the VB_2 surface preventing the contact interaction between La and V borides in the melt. Extended curved LaB_6 «films» (Fig. 1, e) up to 10 μm thick were also observed between some eutectic regions.

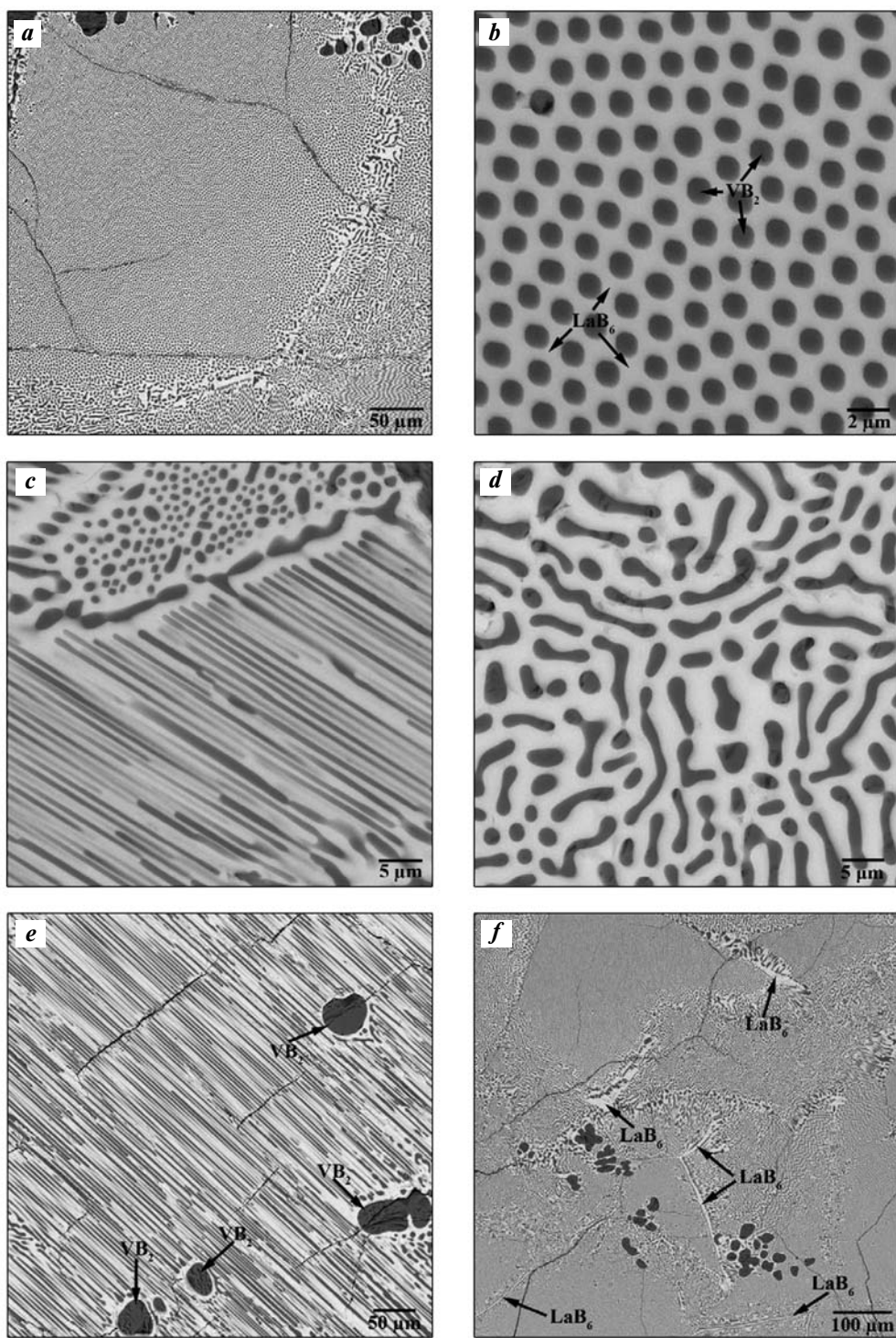


Fig. 1. LaB₆–VB₂ alloy structure (SEM)

a – general view of alloy structure; **b** – area of ordered quasibinary eutectic; **c** – area of quasibinary eutectic with different rod orientation; **d** – area of coarse conglomerate eutectic; **e, f** – areas of quasibinary eutectic with large single-phase VB₂ and LaB₆ inclusions

Рис. 1. Структура сплава LaB₆–VB₂ (СЭМ)

a – общий вид структуры сплава; **b** – область упорядоченной квазибинарной эвтектики; **c** – область квазибинарной эвтектики с различной ориентацией стержней; **d** – область эвтектики грубого конгломерата; **e, f** – области квазибинарной эвтектики с крупными однофазными включениями VB₂ и LaB₆

In addition to the eutectic areas, the alloy contains both VB_2 and LaB_6 crystallization areas. For this reason, we cannot identify whether the composition (eutectic, according to [14, 15]) is in the pre-eutectic or over-eutectic area of the LaB_6 — VB_2 quasi-binary section.

X-ray phase analysis of the alloys confirmed their two-phase composition (Fig. 2). No crystalline phases except for hexagonal VB_2 and cubic LaB_6 were found. The XRD patterns of two mutually perpendicular sections in the crystallized alloys differ in the reflection intensity ratios for different families of lattice planes. It should be noted that the analyzed polished surfaces of *A* and *B* samples contain both transverse and longitudinal sections, and that the ratios of their areas were not equal. Furthermore, due to the above-noted direction of the alloy crystallization temperature gradients, the presence of eutectic regions oriented at arbitrary angles to the polished surface is inevitable.

The abnormally high intensity of (100) and (200) LaB_6 reflexes is strongly pronounced in the XRD pattern *B* in contrast to *A*, where there is a smaller excess over the peak (110) (see Fig. 2), and in which 100 % in-

tensity is standard. For VB_2 , we can note the anomalous intensity of the reflex (100) in pattern *B*. The deviations from the crystallographic standards can be explained by the anisotropic structure of the alloy and the preferential reflection from the corresponding lattice planes.

The LaB_6 and VB_2 phase lattice cell properties are close to their standard values (Table 1). Since there are no significant crystal lattice distortions, this confirms the opinion of S. Ordanyan [14, 15] that LaB_6 and VB_2 are insignificantly soluble in their solid state.

Table 2 lists the concentrations of eutectic alloy components estimated by EDX, IAP, and FP XRD. It also includes the data from [14, 15] for comparison.

The EDX method did not detect the oxygen impurity in the crystallized samples which we detected during the boride powder synthesis. This may be due to the fact that the oxygen was removed as volatile boron suboxide (B_2O_2) during the sample sintering and melting experiment. A silicon carbide impurity content reached 0.7 wt.% after co-milling of boride powders. It was found locally in the peripheral regions of the crystallized alloy. It can be attributed to the gravity separation of the melt since the phase densities are different.

Table 1. Unit cell parameters of LaB_6 and VB_2 phases in the crystallized alloy

Таблица 1. Параметры элементарной ячейки фаз LaB_6 и VB_2 в закристаллизованном сплаве

Phase	Experiment		Standard	
	<i>a</i> , Å	<i>c</i> , Å	<i>a</i> , Å	<i>c</i> , Å
LaB_6	4.1562 ± 0.0005	—	2.1569	—
VB_2	2.9974 ± 0.0005	3.0560 ± 0.0005	29976	3.0562

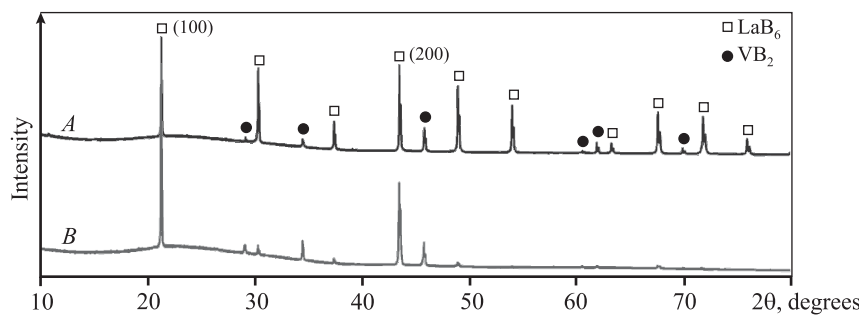


Fig. 2. XRD pattern of LaB_6 — VB_2 alloy

A and *B* – polished sections with predominant content of transverse (*A*) and longitudinal (*B*) VB_2 fiber sections

Рис. 2. Дифрактограмма сплава LaB_6 — VB_2

A и *B* – анишлифы с преимущественным содержанием поперечных (*A*) и продольных (*B*) сечений волокон VB_2

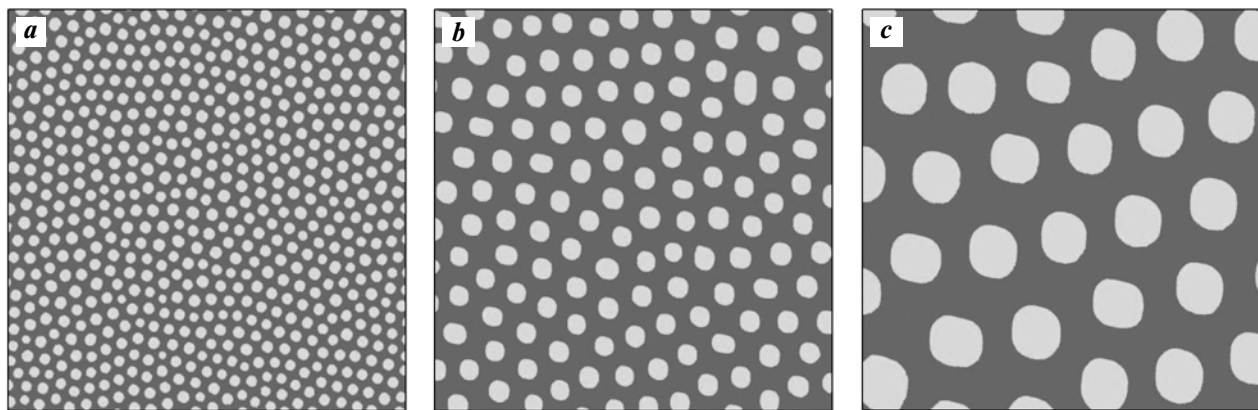


Fig. 3. Example of micrograph binarization for $\text{LaB}_6\text{--VB}_2$ alloy eutectic areas
 $a - \times 4500$, $b - \times 12000$, $c - \times 20000$ magnification

Рис. 3. Пример бинаризации микрофотографий эвтектических областей сплава $\text{LaB}_6\text{--VB}_2$
 a – увеличение $4500\times$, b – $12000\times$, c – $20000\times$

Table 2. Contents of components (mol.%) in $\text{LaB}_6\text{--VB}_2$ eutectic alloy

Таблица 2. Содержание компонентов (моль.%) в эвтектическом сплаве $\text{LaB}_6\text{--VB}_2$

Detection method	LaB_6	VB_2
IAP	42 ± 1	58 ± 1
EDX	38 ± 4	62 ± 4
FP XRD	35 ± 5	65 ± 5
From [14]	31	69
From [15]	35	65

X -ray analysis cannot selectively examine the sample surface. Thus the result characterizes the concentrations of components not only in the eutectic but also in large single-phase regions (see Fig. 1, $d\text{--}e$). This significantly reduces the accuracy of this method as applied to this problem. IAP and EDX methods can select a specific sample region, so they were used to directly analyze the eutectic regions. However, due to the large content of light boron atoms, the component concentration measurement error (MSE) for the EDX method is also high.

Twenty binarized micrographs of the eutectic regions with VB_2 fiber cross sections from different sample sections were taken for multiple IAP measurements (Fig. 3). Statistical processing of the results indicated that the eutectic contains 42 mol.% of LaB_6 and 58 mol.% of VB_2 (1 % MSE).

Conclusion

As a result of the induction melting experiment and subsequent crystallization of the samples made from a mixture of LaB_6 and VB_2 boride powders, alloys with a clear eutectic structure were obtained. The two-phase eutectic regions up to 500 μm are an LaB_6 matrix filled with VB_2 fibers (filamentous, rod-shaped crystals) 0.8–2.0 μm thick. The VB_2 fibers are predominantly oriented along the melt cooling temperature gradient, i.e., from the outer surface to the center.

The alloys contain only two boride phases: cubic LaB_6 ; and hexagonal VB_2 . X -ray methods detected no mutual solubility of the phases.

The comparison of the alloy component concentration measurements by different methods showed that IAP is best suited to measuring eutectic concentration components. The eutectic composition determined by IAP is as follows: 42 \pm 1 mol.% of LaB_6 and 58 \pm 1 mol.% of VB_2 . The discrepancy with the published data is 11 mol.% [14] and 7 mol.% [15].

Acknowledgments: The research was funded by Russian Science Foundation Grant № 19-73-10180.

Исследование выполнено при финансовой поддержке гранта РНФ № 19-73-10180.

References

1. Paderno Y.B., Taran A.A., Voronovich D.A., Paderno V.N., Filipov V.B. Thermionic properties of LaB_6 —

- ($Ti_{0.6}Zr_{0.4}$) B_2 material. *Funct. Mater.* 2008. Vol. 15. No. 1. P. 63. <http://dspace.nbuvg.gov.ua/handle/123456789/137229>.
2. Taran A., Voronovich D., Oranskaya D., Filipov V., Podshyvalova O. Thermionic emission of LaB_6-ZrB_2 quasi binary eutectic alloy with different ZrB_2 fibers orientation. *Funct. mater.* 2013. Vol. 20. No. 4. P. 485–488. DOI: 10.15407/fm20.04.485.
 3. Yang X., Wang P., Wang Z., Hu K., Cheng H., Li Z., Zhang J. Microstructure, mechanical and thermionic emission properties of a directionally solidified LaB_6-VB_2 eutectic composite. *Mater. Design.* 2017. Vol. 133. P. 299–306. DOI: 10.1016/j.matdes.2017.07.069.
 4. Berger M.H., Back T.C., Soukiassian P., Martinotti D., Douillard L., Fairchild S.B., Boeckl J.J., Filipov V., Sayir A. Local investigation of the emissive properties of LaB_6-ZrB_2 eutectics. *J. Mater. Sci.* 2017. Vol. 52. No. 10. P. 5537–5543. DOI: 10.1007/s10853-017-0816-0.
 5. Paderno Y.B., Taran A.A., Ostrovski E.K., Paderno V.N., Filippov V.B. Manufacturing, structure and thermionic properties of lanthanum hexaboride based composite cathode materials. *Funct. mater.* 2001. Vol. 8. No. 4. P. 714–717.
 6. Taran A., Voronovich D., Plankovskyy S., Paderno V., Filippov V. Review of LaB_6 , Re–W dispenser and $BaHfO_3$ –W cathode development. *IEEE Trans. Electr. Devic.* 2009. Vol. 56. No. 5. P. 760–765. DOI: 10.1109/TED.2009.2015615.
 7. Deng H., Dickey E.C., Paderno Y., Paderno V., Filippov V., Sayir A. Crystallographic characterization and indentation mechanical properties of LaB_6-ZrB_2 directionally solidified eutectics. *J. Mater. Sci.* 2004. Vol. 39. No. 19. P. 5987–5994. DOI: 10.1023/B:JMSC.0000041695.40772.56.
 8. Bogomol I., Nishimura T., Vasylkiv O., Sakka Y., Loboda P. High-temperature strength of directionally reinforced LaB_6-TiB_2 composite. *J. Alloys Compd.* 2010. Vol. 505. No. 1. P. 130–134. DOI: 10.1016/j.jallcom.2010.05.003.
 9. Volkova H., Filippov V., Podrezov Y. The influence of Ti addition on fracture toughness and failure of directionally solidified LaB_6-ZrB_2 eutectic composite with monocrystalline matrix. *J. Eur. Ceram. Soc.* 2014. Vol. 34. No. 14. P. 3399–3405. DOI: 10.1016/j.jeurceramsoc.2014.03.018.
 10. Bogomol I., Nishimura T., Nesterenko Y., Vasylkiv O., Sakka Y., Loboda P. The bending strength temperature dependence of the directionally solidified eutectic LaB_6-ZrB_2 composite. *J. Alloys Compd.* 2011. Vol. 509. No. 20. P. 6123–6129. DOI: 10.1016/j.jallcom.2011.02.176.
 11. Chen C.M., Zhang L.T., Zhou W.C. Characterization of LaB_6-ZrB_2 eutectic composite grown by the floating zone method. *J. Cryst. Growth.* 1998. Vol. 191. No. 4. P. 873–878. DOI: 10.1016/S0022-0248(98)00358-3.
 12. Bogomol I., Loboda P. Directionally solidified ceramic eutectics for high-temperature applications. In: *MAX Phases and ultra-high temperature ceramics for extreme environments*. 2013. P. 303. DOI: 10.4018/978-1-4666-4066-5.ch010.
 13. Soloviova T. O., Karasevska O. P., Loboda P. I. Structure, residual stresses and mechanical properties of LaB_6-TiB_2 ceramic composites. *Ceram. Int.* 2019. Vol. 45. No. 7. P. 8677–8683. DOI: 10.1016/j.ceramint.2019.01.189.
 14. Орданъян С.С. О закономерностях взаимодействия в системах $LaB_6-Me^{IV-VI}B_2$. *Неорган. материалы*. 1988. Т. 24. № 2. С. 235–238.
Ordan'yan S.S. About regulations of interaction in $LaB_6-Me^{IV-VI}B_2$ systems. *Neorgan. materialy*. 1988. Vol.24. No 2. P. 235–238 (In Russ.).
 15. Орданъян С.С. Взаимодействие в системах $LaB_6-Me^VB_2$. *Неорган. материалы*. 1984. Т. 20. №. 11. С. 1821–1824.
Ordan'yan S.S. Interaction in $LaB_6-Me^VB_2$ systems. *Neorgan. materialy*. 1984. Vol. 20. No. 11. P. 1821–1824 (In Russ.).
 16. Орданъян С. С., Падерно Ю. Б., Хорошилова И. К., Николаева Е.Е., Максимова Е.В. Взаимодействие в системе LaB_6-ZrB_2 . *Порошк. металлургия*. 1983. №. 11(87). С. 87–90.
Ordan'yan S.S., Paderno Y.B., Khoroshilova I.K., Nikolaeva E.E., Maksimova E.V. Interaction in the LaB_6-ZrB_2 system. *Sov. Powder Metall. Met. Ceram.* 1983. Vol. 22. No. 11. P. 946–948. DOI: 10.1007/BF00805556.
 17. Орданъян С.С., Падерно Ю.Б., Хорошилова И.К., Николаева Е.Е. Взаимодействие в системе LaB_6-HfB_2 . *Порошк. металлургия*. 1984. №. 2 (254). С. 79–81.
Ordan'yan S. S., Paderno Y. B., Khoroshilova I. K., Nikolaeva E.E. Interaction in the LaB_6-HfB_2 system. *Sov. Powder Metall. Met. Ceram.* 1984. P. 23. No. 2. P. 157–159. DOI: 10.1007/BF00792275.
 18. Орданъян С.С., Падерно Ю.Б., Николаева Е.Е., Хорошилова И.К. Взаимодействие в системе LaB_6-CrB_2 . *Порошк. металлургия*. 1984. Т. 257. №. 5. С. 64–66.
Ordan'yan S.S., Paderno Y.B., Nikolaeva E.E., Khoroshilova I.K. Interaction in the LaB_6-CrB_2 system. *Powder*

- Metall. Met. Ceram.* 1984. Vol. 23. No. 5. P. 387–389.
DOI: 10.1007/BF00796605.
19. Орданьян С.С., Несмелов Д.Д., Вихман С.В. Взаимодействие в системе LaB₆—W₂B₅. *Неорган. материалы*. 2009. Т. 45. №. 7. С. 1–4.
Ordan'yan S.S., Nesmelo D.D., Vikhman S.V. Phase relations in the LaB₆—W₂B₅ system. Inorg. Mater. 2009. Vol. 45. No. 7. P. 754–757. DOI:10.1134/S0020168509070097.
20. Лобода П.И., Кисла Г.П., Богомол И.И., Сысоев М.А., Карасевская О.П. Фазовые равновесия в системе LaB₆—MoB₂. *Неорган. материалы*. 2009. Т. 45. №. 3. С. 288–291.
Loboda P.I., Kisla G.P., Bogomol I.I., Sysoev M.A., Karasevskaya O.P. Phase relations in the LaB₆—MoB₂ system. Inorg. Mater. 2009. Vol. 45. No. 3. P. 246–249. DOI: 10.1134/S0020168509030042.
21. Kysla G., Loboda P. Ceramic materials of the quasi-binary LaB₆—MoB₂ system. *Process. Appl. Ceram.* 2007. Vol. 1. No. 1-2. P. 19–22. DOI: 10.2298/PAC0702019K.
22. Бешта С.В., Крушинов Е.В., Альмашев В.И., Витоль С.А., Мезенцева Л.П., Петров Ю.Б., Лопух Д.Б., Хабенский В.Б., Баррачин М., Хеллманн З., Гусаров В.В. Фазовые соотношения в системе ZrO₂—FeO. *Журн. неорган. химии*. 2006. Т. 51. №. 2. С. 367–374.
Beshta S.V., Krushinov E.V., Al'myashhev V.I., Vitol' S.A., Mezentseva L.P., Petrov Yu.B., Lopukh D.B., Khabenskii V.B., Barrachin M., Hellmann S., Gusalov V.V. Phase relations in the ZrO₂—FeO system. Russ. J. Inorg. Chem. 2006. Vol. 51. No. 2. P. 325–331. DOI: 10.1134/S0036023606020227.
23. Несмелов Д.Д., Новоселов Е.С., Вихман С.В. Кристаллизация эвтектических структур в системе LaB₆—W₂B₅—NbB₂. *Физика и химия стекла*. 2022. Vol. 48. No. 1. P. 34–43. DOI: 10.31857/S0132665122010097.
Nesmelo D.D., Novoselov E.S., Vikhman S.V. Crystallization of eutectic structures in the LaB₆—W₂B₅—NbB₂ system. Glass Phys. Chem. 2022. Vol. 1. No.1. P. 23–29. DOI: 10.1134/S1087659622010096.